New Journal of Physics
The open access journal at the forefront of physics

Deutsche Physikalische Gesellschaft DPG
IOP Institute of Physics

Published in partnership with: Deutsche Physikalische Gesellschaft and the Institute of Physics

OPEN ACCESS

RECEIVED
30 November 2018

REVISED
9 April 2019

ACCEPTED FOR PUBLICATION
23 April 2019

PUBLISHED
22 May 2019

PAPER

Realising single-shot measurements of quantum radiation reaction in high-intensity lasers

C D Baird[1], C D Murphy[1], T G Blackburn[2,5], A Ilderton[3], S P D Mangles[4], M Marklund[2,5] and C P Ridgers[1]

[1] York Plasma Institute, Department of Physics, University of York, Heslington, York YO10 5DQ, United Kingdom
[2] Department of Physics, Chalmers University of Technology, SE-41296 Gothenburg, Sweden
[3] Centre for Mathematical Sciences, University of Plymouth, PL4 7AA, United Kingdom
[4] Blackett Laboratory, Imperial College London, South Kensington, London SW7 2BZ, United Kingdom
[5] Present address: Department of Physics, University of Gothenburg, SE-41296 Gothenburg, Sweden

E-mail: cdb525@york.ac.uk

Keywords: radiation reaction, laser-plasma interactions, inverse Compton scattering, QED plasma

Abstract

Modern laser technology is now sufficiently advanced that collisions between high-intensity laser pulses and laser-wakefield-accelerated (LWFA) electron beams can reach the strong-field regime, so that it is possible to measure the transition between the classical and quantum regimes of light–matter interactions. However, the energy spectrum of LWFA electron beams can fluctuate significantly from shot to shot, making it difficult to clearly discern quantum effects in radiation reaction (RR), for example. Here we show how this can be accomplished in only a single laser shot. A millimetre-scale pre-collision drift allows the electron beam to expand to a size larger than the laser focal spot and develop a correlation between transverse position and angular divergence. In contrast to previous studies, this means that a measurement of the beam's energy-divergence spectrum automatically distinguishes components of the beam that hit or miss the laser focal spot and therefore do and do not experience RR.

1. Introduction

Bright, energetic radiation is produced across the electromagnetic spectrum when high-intensity lasers irradiate matter, due to the violent acceleration of electrons induced by the laser fields [1]. The next generation of lasers will be sufficiently intense that recoil forces from this emission, known as radiation reaction (RR), will dominate the dynamics of the plasmas they create [2–6]. When the energy of an individual photon of the emitted radiation becomes comparable to that of the electron, we must account for quantum effects on RR, for which there is no complete theoretical description (in the highly multiphoton regime where the electron interacts with $\gg 1$ laser photon) [7, 8]. This makes experimental validation of current models of quantum RR crucial to our understanding of the behaviour of plasmas created by next generation lasers, and to realising their many applications, which include hard x-ray sources [9–12], compact electron accelerators [13–17] and ion acceleration [18–22]. For example recent work has shown that quantum RR leads to almost complete laser absorption [23] which may substantially reduce the energy of accelerated ions [24, 25].

The peak intensities of current laser systems ($\sim 10^{21}$ W cm^{-2}) are not sufficient to elicit RR effects in stationary targets. However, by pre-accelerating electrons to GeV-scale energies, for example, by laser wakefield acceleration [26–29], RR regimes become accessible. The geometry required is similar to experiments previously used to probe Thomson and Compton scattering in the nonlinear regime [11, 30–32], see figure 1. Recent experiments have shown that detection of RR is achievable on current facilities [33, 34]; however due to the shot-to-shot variation of both the electron bunch and the colliding laser pulse, it was not possible to clearly distinguish between classical and quantum (stochastic) effects on the electron motion. Here we propose a solution to this problem by incorporating a pre-interaction drift which causes the electron's transverse

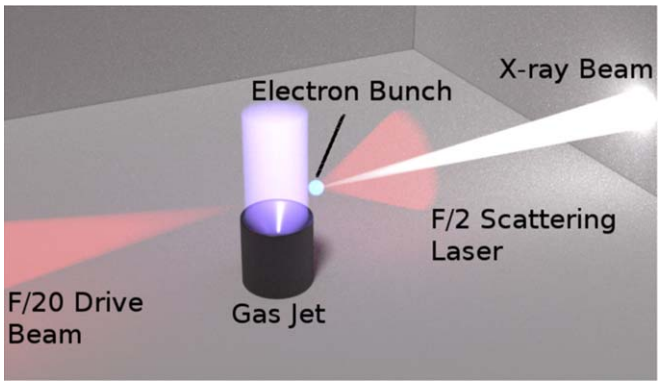

Figure 1. A schematic of an all-optical inverse Compton scattering setup. An $F/20$ drive laser (intensity $\sim 10^{19}$ W cm^{-2}) is focused into a supersonic gas jet, producing an electron bunch via wakefield acceleration. These electrons then collide with a counter-propagating $F/2$ laser pulse (of high intensity $\sim 10^{21}$ W cm^{-2}). The scattered electrons produce a bright x-ray beam.

momentum to become correlated to their transverse position in the bunch. After the collision, the electrons retain their initial spectral characteristics at the edges, allowing for on-shot comparison of the pre- and post-interaction spectra.

The importance of quantum effects on RR is quantified by the parameter

$$\chi = \frac{\gamma\sqrt{(\vec{E} + \vec{v} \times \vec{B})^2 - (\vec{v} \cdot \vec{E})^2}}{E_{\text{crit}}} \simeq 0.1 \frac{\gamma}{1000} \frac{a_0}{20} \left(\frac{\lambda_L}{\mu\text{m}} \right)^{-1}, \tag{1}$$

where the electron has velocity $\vec{v}$ and Lorentz factor γ, $E_{\text{crit}} = 1.38 \times 10^{18}$ V m^{-1} is the critical field of QED [35], and λ and a_0 are the laser wavelength and strength parameter, related to the laser intensity through $I_0 = (\pi c/2)(m_e c^2 a_0 / e\lambda_L)^2$.

χ may be interpreted as the electric field in the rest frame of the radiating electron or positron in units of E_{crit}, hence the increased importance of quantum effects when the electrons are accelerated to high energies in the counter-propagating geometry shown in figure 1. The Lorentz boost for an ultra-relativistic electron in this configuration increases the apparent strength of the laser electromagnetic fields, and so χ. The final expression in (1) is valid for this specific geometry. As χ approaches unity, RR must be described in a quantum framework. For $\chi \sim 0.1$, the energy of emitted photons becomes a significant fraction of the emitting electron's energy and photon emission becomes stochastic [36], rather than continuous as in the classical case. Equation (1) demonstrates that to reach $\chi > 0.1$, at a peak intensity of $I = 10^{21}$ W cm^{-2} one needs electrons with $E > 500$ MeV.

Quantum corrections to the radiation spectrum, which guarantee that no photon is emitted with energy greater than the electron, reduce the power emitted compared to the classical case [37].

The stochastic nature of the emission means that the electrons may move into classically inaccessible regions of phase space [38, 39]: in the colliding beams scenario, quantum effects can lead to a broadening of the energy spectrum where a classical treatment can only result in narrowing [40–44], increased emission of hard photons [36], a transverse broadening of the electron bunch [45] and 'quenching' of emission [46]. See [47] for quantum effects beyond stochasticity.

In order to measure RR effects in electron spectra, it is important that significant damping occurs during the interaction. We define 'strong' RR to correspond to an electron losing 10% of its initial energy per laser cycle, i.e. operating in the radiation-dominated regime [48]. Following the work of Thomas *et al* [49] we use the parameter ψ to characterise the regime, where strong RR occurs for $\psi > 1$. In the interaction of an electron beam with a counter-propagating laser pulse, we can predict the required parameters from the condition $\psi \coloneqq 0.12(\gamma/1000)(a_0/10)^2 > 1$. Therefore, if $\gamma > 1000$ ($E_{e^-} > 500$ MeV) and $a_0 > 30$ we reach the regime of strong RR.

Although the counter-propagating geometry is promising for measurement of quantum effects on RR, shot-to-shot variation of the electron energy can prevent such experiments from reaching the finesse required for unambiguous identification of stochastic effects. In this paper we will explore the possibility of overcoming this by using the aforementioned pre-interaction drift using QED-particle in cell (QED-PIC) simulations. We will see that, given sensitive enough detectors to measure the electron energy spectrum, this could provide a relatively simple solution to this problem.

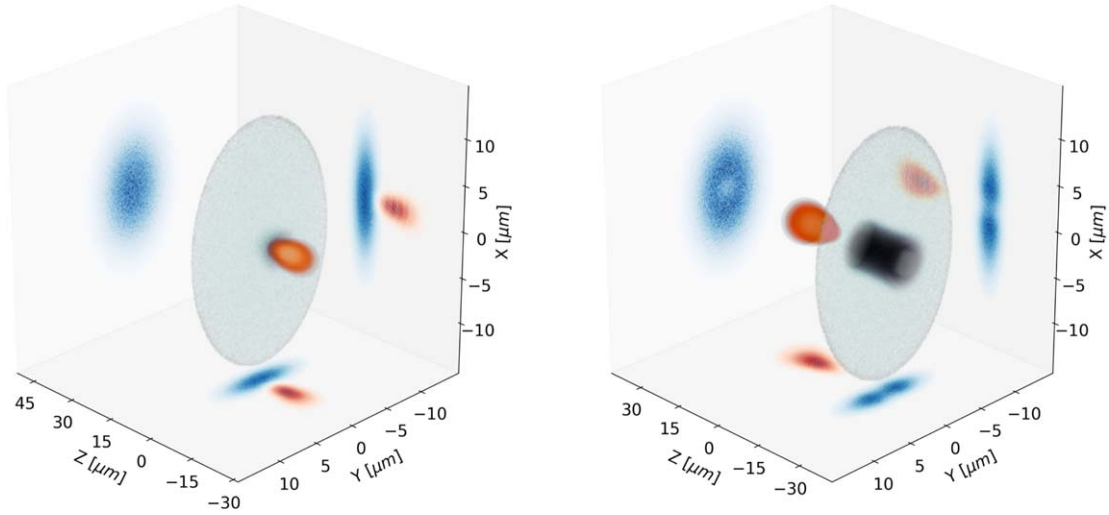

Figure 2. Simulation data showing the laser pulse as it focuses through the centre of the electron bunch. The dark region indicates where electrons have lost energy due to radiation reaction. The cross-sections show the electron energy density (blue) and the laser intensity profile (red). Simulation performed using EPOCH. The spatial grid resolution was 10 cells per micron and the electron bunch was represented by 10^8 macro-particles.

2. QED-PIC simulations

We model quantum effects, including RR, using the now-standard approach based on the 'locally constant field approximation'. The basic assumption is that at high intensity the formation time of any quantum process is so short that it may be treated as an instantaneous event occurring in a field which is effectively constant. This allows quantum processes to be incorporated into classical particle-in-cell (PIC) codes as stochastic emission events. For a review see [50]. This model has been implemented within the three-dimensional PIC code EPOCH [51], using a Monte Carlo algorithm. Details of the implementation can be found in [52].

We simulated the interaction of an energetic electron bunch with a counter-propagating, high-intensity laser using EPOCH. The bunch had a central energy of 1 GeV, with an rms spread of 50 MeV. It was distributed according to a 3D Gaussian number density profile with a peak of 1.87×10^{23} m^{-3} and e-folding distances of $6 \times 4 \times 4$ microns in the x, y and z directions respectively, where the laser was polarised in the x direction. This elongated shape was specifically chosen to model the known spreading of laser-wakefield-generated bunches in the laser polarisation direction [53]. The divergence profile of the bunch was taken to be a Gaussian shape, with FWHM of 5 mrad in both transverse directions. The laser parameters were chosen to model a potential experiment on the Astra Gemini laser [54]. The laser pulse propagated in the z direction, focused to a diffraction-limited spot of width 2 μm and had a peak focused intensity of 1×10^{21} W cm^{-2}, a pulse length of 44 fs ($1/e^2$ in intensity) and a central wavelength of 800 nm, which equates to an a_0 of 21.5. The interaction is shown visually in figure 2.

In the simulations we varied the distance the electron bunch propagated before the interaction, which we refer to as 'drift'. At the electron beam 'waist' (the minimum beam diameter) the electrons at each transverse position (x) can have a range of transverse momenta, and therefore propagate at a range of angles θ. After a drift, electrons with large θ are at a larger transverse position x, while those with low θ remain close to the axis. If the drift length is long enough, this correlation dominates over the initial spread of position. This drift was incorporated into the simulations by first initialising, and then redistributing the electrons by extrapolating their starting positions based on the divergence angle (neglecting space charge effects), i.e. $x_f = x_i + d(p_x/p_z)$, where d is drift. With these initial conditions, we reach $\psi \simeq 1$, corresponding to the radiation dominated regime [49]. Further, $\chi \simeq 0.25$ for the interaction, so quantum RR effects will be present.

Our choice of electron spectrum is motivated by recent results [55–57] which present experimentally-produced laser-wakefield-accelerated (LWFA) beams with similar characteristics, i.e. GeV-scale with a low energy spread of ~10%.

Figure 3 shows the electron spectrum immediately following the interaction. Around 50% of the electrons have emitted hard photons and as a result experienced RR, lowering the peak and introducing a long, low energy tail into the spectrum. The discrepancy between the classical model (based on the Landau–Lifshitz equation [58, 59]) and QED is most apparent in the low-energy region.

Figure 4 shows phase-space representations of the electron bunch before, figure 4(a), and immediately after the interaction, figure 4(b). It can be seen that the central region of the electron bunch, i.e. where the bunch

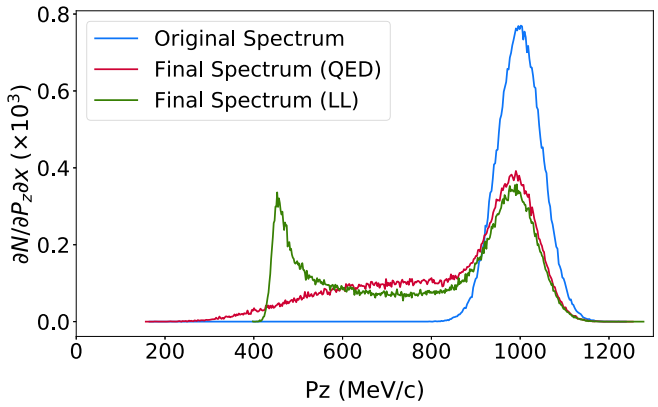

Figure 3. Initial electron spectrum (blue), alongside the post-interaction spectra including QED effects (red). The emission process causes significant recoil in the electron population, resulting in a decrease in energy and an increase in spread. The classical prediction (green), using the Landau–Lifshitz model, shows bunching of the electrons at the low-energy end, as expected.

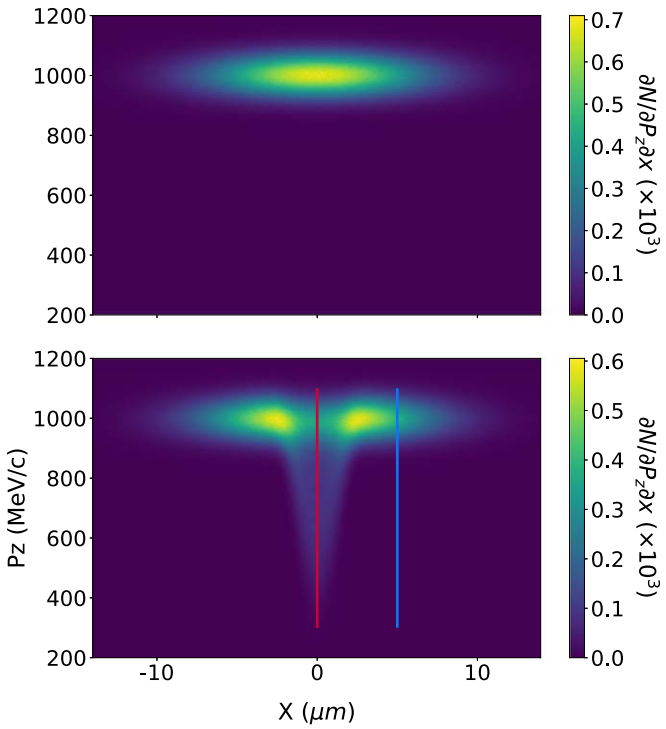

Figure 4. Phase space representation of the electron bunch before (a) and after (b) interaction with the laser pulse; there is a significant shift to lower energy in the central region marked by the red line, whereas the edge regions (blue line) have not interacted. Modelled using quantum radiation reaction.

overlaps with the laser pulse, has experienced RR, resulting in a long tail of low energy electrons. The edges of the electron bunch, however, have remained unchanged since the width of the electron bunch is larger than that of the focused laser pulse. The fact that the central region of the image gives the electron spectrum after interaction and the edge regions retain the original electron spectrum would, crucially, allow us to determine the effect of RR on the spectrum on a shot-by-shot basis, regardless of variations in the pre-interaction spectrum.

The characteristics of the 'depletion zone' in the interaction region have been investigated by Blackburn (2015) [60]. In the following sections we will extend this work by exploring the possibility of direct experimental measurement of this region.

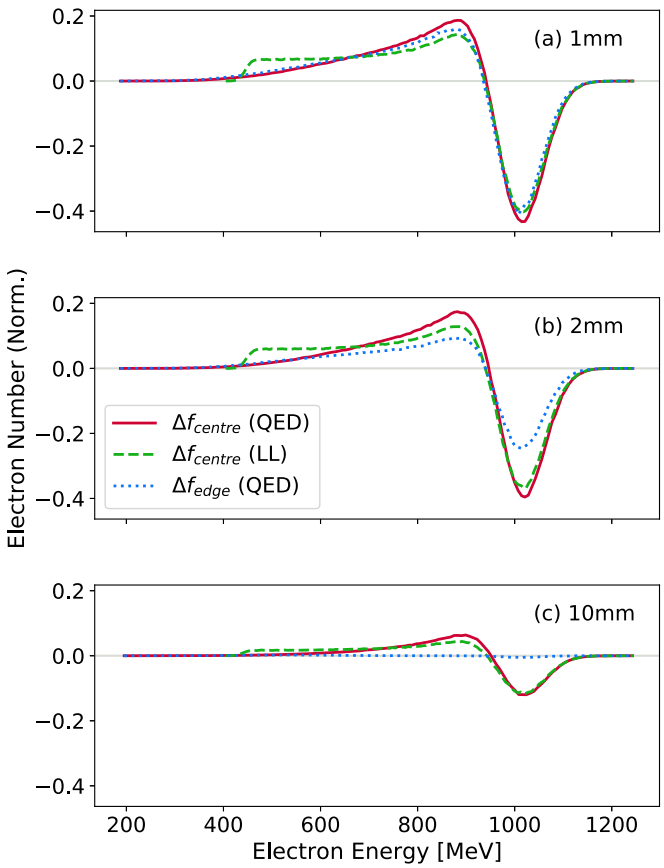

Figure 5. Electron energy spectra taken from the central region (red), and the edge region (blue). The central region from the LL interaction is also shown (green). The profiles shown are generated by subtracting the spectrum with no laser interaction (laser off), from that with laser interaction (laser on). The initial drift distance is (a) 1 mm; (b) 2 mm; (c) 10 mm. It can be seen that, at $d = 10$ mm, the edge spectrum (blue) closely resembles that of the original; however, the signal in the centre is also reduced. The edge spectrum from the LL interaction is not shown for clarity, but follows the same pattern as the QED interaction.

3. Experimental constraints

In a real experiment the electron spectrum cannot be measured immediately after the interaction. Resolving the energy spectrum of the bunch requires propagation through a spectrometer magnet, the length of which may extend for tens of centimetres. Moreover, the screen must be placed some distance from the magnet to optimise energy resolution (usually a metre or more). Over this distance, the divergence of the electron bunch, as well as the additional effect of ponderomotive scattering, causes the spectrum to blur such that the shifted electrons spread across the full width of the bunch.

We can, however, solve this problem by varying the initial drift in the manner discussed above. Increasing the drift distance has the effect of reducing the divergence in the central region, where the interaction occurs, and thus the large propagation distance through a spectrometer causes less blurring of the spectrum. The spectrum in the central region then retains the signature of RR, whereas the edge spectrum resembles the original, as desired.

To confirm that the edge region does indeed represent the original, we compare the post-interaction spectra at the centre and edge of the bunch, f_{laser}, to control spectra taken from an electron bunch which has not interacted with the laser, $f_{\text{no laser}}$. We expect that the spectrum at the edge of the screen should match the pre-interaction spectrum, allowing us to contrast it with the spectrum at the centre. It can be seen in figure 5 that as the initial propagation distance, d, increases, the edge spectrum does indeed tend toward that of the control, i.e. pre-interaction, spectrum (so $\Delta f := f_{\text{laser}} - f_{\text{no laser}} \simeq 0$). Furthermore, comparison with the central region shows that the signature of the interaction is indeed retained in the spectrum, albeit reduced somewhat due to the decreased electron density as the bunch propagates.

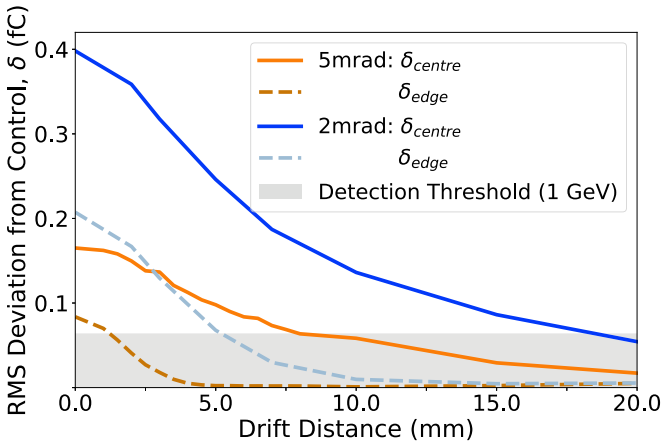

Figure 6. Plot of the values of δ in the central and edge regions as a function of drift distance for initial beam divergence of 5 mrad (orange lines) and 2 mrad (blue lines). The optimum drift distance occurs when δ_{edge} falls below the detector threshold of $\sim$10 fC mm^{-2}. The detector threshold shown is for high-sensitivity image plate as in [61].

4. Optimum drift distance

There are two competing effects in play here; the divergence of the electron bunch causes it to expand as it propagates, and so the fraction of electrons in the interaction region decreases as a function of distance travelled, while the correlation between (transverse) position and momentum increases with distance. Indeed, figure 5(c) indicates that detection of RR, and particularly distinguishing between quantum and classical effects, may become difficult if the drift distance is too long. This suggests that there is an optimum drift distance where the fraction of electrons interacting is sufficient for measurement, but also where the original spectrum can be deduced from the edges of the bunch. Identifying this optimum distance would maximise our ability to measure the effect of RR shot-to-shot.

To identify the optimum distance, and understand how it is affected by the initial parameters of the electron bunch, we look at how the spectrum deviates from the pre-interaction control spectrum. We take the rms deviation-from-control, $\delta := \sqrt{\overline{(\Delta f)^2}}$, for the central (interaction) region, and also for the edge region. Figure 6 shows the variation of δ in the central and edge regions as a function of drift distance d.

As the drift distance increases, the value of δ falls both in the centre (δ_{centre}) and at the edge (δ_{edge}) of the screen. When $\delta_{\text{edge}} \simeq 0$, the post-interaction spectrum at the edge is indistinguishable from the pre-interaction spectrum, and so we can compare it to the central spectrum to determine how RR affects the spectrum shot-to-shot. Considering the experimental realisation of this measurement, we can be less strict and assume that the optimum drift distance occurs where the value of δ_{edge} falls below the detection threshold of our spectrometer screen. (Similarly, the maximum drift distance is determined by the value of δ_{centre}, i.e. any spectral shift ceases to be measurable below the detection threshold.)

Studies of various types of image plate [61] have found a lower detection threshold of around 10 fC mm^{-2}. Using this, we can estimate the value of δ_{edge} below which the spectrum is the same as the pre-interaction spectrum to within the limits of the detector.

To quantify the detector threshold, we considered the motion of electrons through a 30 cm, 1 T uniform magnetic field, to a screen located 70 cm from the exit of the magnet. This setup approximately matches the spectrometer geometry at the Astra Gemini facility. We then used the dispersion of the electrons to transform energy values on the spectrum into positional values on the screen. By translating the value of δ into an areal density of electrons, we can directly compare it to the detection threshold: this yields the grey-shaded region in figure 6. As seen in the figure, the optimum drift distance is between 1 and 6 mm for an initial divergence of 5 mrad (FWHM), and between 5 and 17 mm for a 2 mrad (FWHM) divergence. The rms deviation from control is on the order of 1000 electrons, thus is likely to present difficulties for a low-sensitivity detector, such as lanex; and indeed even for a sensitive image plate if beam divergence is high. Other, more sensitive detection methods may prove invaluable in measuring this effect.

By considering the geometry of the electron propagation, we can obtain an estimate for the optimum drift distance for arbitrary divergence angles. The preservation of the depletion zone depends on establishing a correlation in $x - p_x$ phase space. For this to occur, the electrons initially in the 'wrong' position, i.e. top-left (bottom right) of figure 7, must propagate to the top-right (bottom-left). Spatially, this requires the electron to travel the width of the electron bunch.

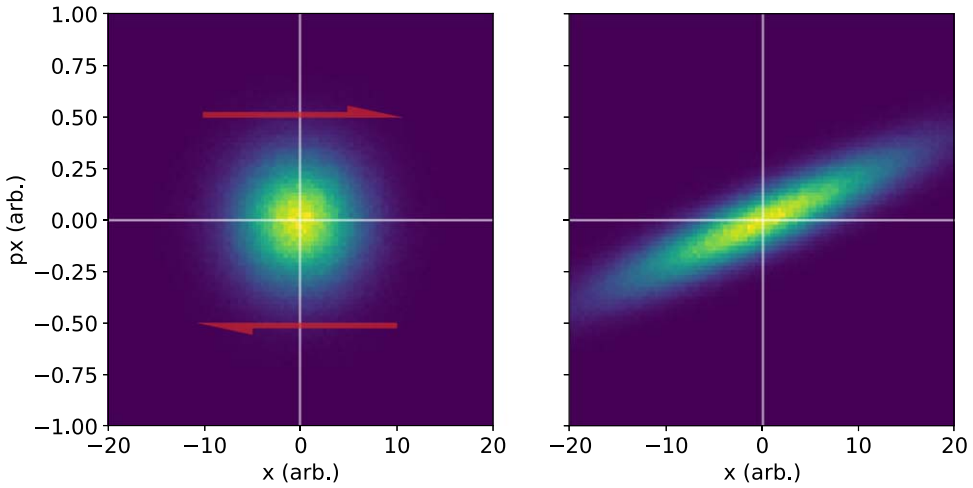

Figure 7. Schematic of $x - p_x$ phase space. The initially uncorrelated electrons (left) become progressively more correlated as they propagate (right).

For an electron bunch with rms divergence θ, and width w_e, the minimum drift distance d_{min} is

$$d_{\mathrm{min}} \sim \frac{w_e}{\theta}. \tag{2}$$

In the two cases discussed above, $\theta = 0.9$ mrad (2 mrad FWHM) and $\theta = 2.1$ mrad (5 mrad FWHM), this yields $d_{\mathrm{min}} \sim 11$ mm and $d_{\mathrm{min}} \sim 4.8$ mm. This estimate does not, of course, take into account the detection threshold, which is dependent on the spectrometer configuration.

5. Discussion

A major barrier to the measurement of quantum effects on RR in a collider setup (as shown in figure 1) is the shot-to-shot fluctuation of the electron energy spectrum. This prevents comparison with the currently accepted quantum model, based on the locally constant field approximation, with the required finesse to determine its accuracy [33, 34]. One solution to this would be to use a conventional particle accelerator to provide the electron beam. Conventional accelerators produce substantially more reproducible, lower energy spread beams than those from laser wakefield acceleration. However, to perform experiments in the highly multi-photon regime the counter-propagating laser pulse must have intensity $\gg 10^{18}$ W cm^{-2} and as yet there is no conventional accelerator facility co-located with a laser of the required intensity. In addition, the femtosecond duration of LWFA electron beams and intrinsic synchronisation of the electron beam and colliding laser in twin-beam systems, e.g. Astra Gemini, makes an all-optical setup more convenient than a conventional accelerator-based approach. Another alternative is to use an aligned crystal lattice to provide the strong fields, although in this case the a_0 is fixed by the nuclear field strength. This alternative approach has recently produced interesting results although again definitive model comparison is a challenge [62].

Here we have shown that another solution is possible where we can measure the pre and post-interaction electron energy spectrum on the same laser shot, meaning that the shot-to-shot variation is no longer important. To do this we require that the electron bunch drifts some distance in order that correlation of the transverse momentum of the electrons develops across the bunch. We found that the optimum drift distance was dependent on the angular divergence of the electron beam (lower divergence beams must drift further to develop a given degree of correlation) and that a drift of 5–10 mm was optimal; if the beam drifts too far it becomes too large such that the counter-propagating laser interacts with only a small fraction of the electrons and the signal-to-noise at the detector becomes too low. We have used an azimuthally-symmetric divergence profile, so that the electron bunch expands equally in both axes as it drifts. In this case the result is independent of the transverse axis used for the measurement. Experimentally however, a variation in the ratio θ_x/θ_y will change the fraction of electrons in the interaction region, and may alter the optimum drift distance.

It should be noted that this technique relies on assumptions about the distribution of the electrons in phase space after laser wakefield acceleration. How well this is known is an open and pertinent question. We have accounted for the fact that the electron bunch is usually elongated along the laser polarisation axis [53]. The details of this elongation are important as it determines the transverse size of the electron bunch (on exiting the wakefield accelerating region, which itself may not be well known but can be relatively reliably inferred from

simulations) which in turn determines the signal-to-noise on collision with the counter-propagating laser pulse. We have assumed that the transverse momentum of the electrons is initially uncorrelated to their position. This is reasonable as strong correlation would be readily observable in current experiments, but is not. We have also assumed that there is no correlation of divergence angle with electron energy. Such correlation would mean that the spectrum at the edge of the electron bunch after drifting, would no longer be representative of the pre-interaction spectrum. Theoretical calculations [63, 64] indicate that a weak coupling occurs, scaling with $p_z^{1/4}$. Incorporating this into our simulations, we find that the difference between the spectra is significantly smaller than the total signal and does not constitute a serious impediment to the measurement.

Previous experiments have used different approaches to overcome the problem of shot-to-shot variation of the electron beam. Use of a gas-cell target [34], for example, improves the stability of the electron beam, but it is unlikely that fluctuations in the electron energy can be completely eliminated. There is also a question about the timing of the collision of the electron bunch with the laser pulse, leading to uncertainty in the value of a_0 at collision. This is circumvented by our new method of drift as in principle the laser pulse intensity profile is imprinted on the electron bunch. An alternative is to accept the variation and use a statistical approach [33]. This requires many collision shots to allow accurate comparison between models, which is difficult to achieve. In addition while the average energy of the electron bunch may be stable enough for useful data to emerge from the statistical noise, the shape of the spectrum may not be (for example see [33], figure 4), which can limit the detection of stochastic quantum effects [43, 44, 65]. The importance of quantum RR in next generation multi-PW laser-plasma interactions necessitates extensive testing of the models of this process in QED-PIC codes and therefore novel methods for overcoming the major difficulties in experiments to do this, such as that presented here.

6. Conclusions

In this paper we have presented a new approach to the experimental measurement of quantum RR effects in an inverse Compton scattering arrangement. In our setup, the electron bunch is, by design, larger than the focused laser pulse. By allowing the bunch to propagate for a short distance between production and interaction, we establish a correlation between transverse position and momentum of the electrons. This preserves the transverse structure of the bunch during transport to the spectrometer screen, allowing measurement of the post-interaction spectrum in the centre of the bunch, and the pre-interaction spectrum at the edge. Although detection of the spectral shift is made challenging due to the small number of electrons involved, it should be possible with sensitive image plates, or other detectors with close to single-particle detection efficiency.

CDB, CPR and CDM would like to acknowledge funding from EPSRC grant EP/M018156/1. TGB and MM acknowledge support from the Knut and Alice Wallenberg Foundation. MM acknowledges support from the Swedish Research Council, grants 2013-4248 and 2016-03329. SPDM acknowledges funding from EPSRC grant EP/M018555/1 and ERC grant 682399.

ORCID iDs

C D Baird https://orcid.org/0000-0001-9973-7173
C D Murphy https://orcid.org/0000-0003-3849-3229
T G Blackburn https://orcid.org/0000-0002-3681-356X
A Ilderton https://orcid.org/0000-0002-6520-7323
S P D Mangles https://orcid.org/0000-0003-2443-4201
M Marklund https://orcid.org/0000-0001-9051-6243
C P Ridgers https://orcid.org/0000-0002-4078-0887

References

[1] Corde S *et al* 2013 *Rev. Mod. Phys.* **85** 1
[2] Bell A R and Kirk J G 2008 *Phys. Rev. Lett.* **101** 200403
[3] Tamburini M, Pegoraro F, Di Piazza A, Keitel C H and Macchi A 2010 *New J. Phys.* **12** 123005
[4] Bulanov S V *et al* 2011 *Nucl. Instrum. Methods Phys. Res.* A **660** 31
[5] Ridgers C P *et al* 2012 *Phys. Rev. Lett.* **108** 165006
[6] Ridgers C P *et al* 2013 *Phys. Plasmas* **20** 056701
[7] Ritus V I 1985 *J. Sov. Laser Res.* **6** 497
[8] Di Piazza A, Müller C, Hatsagortsyan K Z and Keitel C H 2012 *Rev. Mod. Phys.* **84** 1177
[9] Kneip S *et al* 2010 *Nat. Phys.* **6** 980
[10] Ta Phuoc K *et al* 2012 *Nat. Photon.* **6** 308
[11] Chen S *et al* 2013 *Phys. Rev. Lett.* **110** 155003

[12] Powers N D et al 2013 Nat. Photon. 8 28
[13] Tajima T and Dawson J M 1979 Phys. Rev. Lett. 43 267
[14] Ting A et al 1997 Phys. Plasmas 4 1889
[15] Amiranoff F et al 1998 Phys. Rev. Lett. 81 995
[16] Malka V et al 2002 Science 298 1596
[17] Mangles S P D et al 2004 Nature 431 535
[18] Schwoerer H, Liesfeld B, Schlenvoigt H, Amthor K and Sauerbrey R 2006 Phys. Rev. Lett. 96 014802
[19] Snavely R A et al 2000 Phys. Rev. Lett. 85 2945
[20] Hatchett S P et al 2000 Phys. Plasmas 7 2076
[21] Zepf M et al 2003 Phys. Rev. Lett. 90 064801
[22] McKenna P et al 2007 Plasma Phys. Control. Fusion 49 B223
[23] Zhang P, Ridgers C P and Thomas A G R 2015 New J. Phys. 17 043051
[24] Sorbo D D et al 2018 New J. Phys. 20 033014
[25] Duff M J et al 2018 Plasma Phys. Control. Fusion 60 064006
[26] Leemans W P et al 2006 Nat. Phys. 2 696
[27] Kneip S et al 2009 Phys. Rev. Lett. 103 035002
[28] Clayton C E et al 2010 Phys. Rev. Lett. 105 105003
[29] Leemans W P et al 2014 Phys. Rev. Lett. 113 245002
[30] Chen S, Maksimchuk A and Umstadter D 1998 Nature 396 653
[31] Sarri G et al 2014 Phys. Rev. Lett. 113 224801
[32] Yan W et al 2017 Nat. Photon. 11 514
[33] Cole J M et al 2018 Phys. Rev. X 8 11020
[34] Poder K et al 2018 Phys. Rev. X 8 031004
[35] Sauter Z 1931 Physics 69 742
[36] Blackburn T G, Ridgers C P, Kirk J G and Bell A R 2014 Phys. Rev. Lett. 112 015001
[37] Erber T 1966 Rev. Mod. Phys. 38 626
[38] Shen C S and White D 1972 Phys. Rev. Lett. 28 455
[39] Duclous R, Kirk J G and Bell A R 2011 Plasma Phys. Control. Fusion 53 015009
[40] Neitz N and Di Piazza A 2013 Phys. Rev. Lett. 111 054802
[41] Yoffe S R, Kravets Y, Noble A and Jaroszynski D A 2015 New J. Phys. 17 053025
[42] Vranic M, Grismayer T, Fonseca R A and Silva L O 2016 New J. Phys. 18 053025
[43] Ridgers C P et al 2017 J. Plasma Phys. 83 715830502
[44] Niel F, Riconda C, Amiranoff F, Duclous R and Grech M 2018 Phys. Rev. E 97 043209
[45] Green D G and Harvey C N 2014 Phys. Rev. Lett. 112 164801
[46] Harvey C N, Gonoskov A, Ilderton A and Marklund M 2017 Phys. Rev. Lett. 118 105004
[47] Dinu V, Harvey C, Ilderton A, Marklund M and Torgrimsson G 2016 Phys. Rev. Lett. 116 044801
[48] Koga J, Esirkepov T Z and Bulanov S V 2005 Phys. Plasmas 12 093106
[49] Thomas A G R, Ridgers C P, Bulanov S S, Griffin B J and Mangles S P D 2012 Phys. Rev. X 2 041004
[50] Gonoskov A et al 2015 Phys. Rev. E 92 023305
[51] Arber T D et al 2015 Plasma Phys. Control. Fusion 57 113001
[52] Ridgers C P et al 2014 J. Comput. Phys. 260 273
[53] Mangles S P D et al 2006 Phys. Rev. Lett. 96 215001
[54] Hooker C J et al 2006 J. Phys. IV 133 673
[55] Wang X et al 2013 Nat. Commun. 4 1988
[56] Kim H T et al 2013 Phys. Rev. Lett. 111 165002
[57] Mirzaie M et al 2015 Sci. Rep. 5 14659
[58] Landau L D and Lifshitz E M 1975 The Classical Theory of Fields (Amsterdam: Elsevier)
[59] Burton D A and Noble A 2014 Contemp. Phys. 55 110
[60] Blackburn T G 2015 Plasma Phys. Control. Fusion 57 075012
[61] Buck A et al 2010 Rev. Sci. Instrum. 81 033301
[62] Wistisen T N, Di Piazza A, Knudsen H V and Uggerhøj U I 2018 Nat. Commun. 9 795
[63] Reitsma A J W and Jaroszynski D A 2004 Laser Part. Beams 22 407
[64] Thomas A G R 2010 Phys. Plasmas 17 056708
[65] Vranic M, Martins J L, Fonseca R A and Silva L O 2016 Comput. Phys. Commun. 204 141